

where

$$\frac{1}{m^*(\mathcal{E})} = 2 \sum_{\mu} \left[\frac{\pi_{j\mu}^x \pi_{\mu j}^x}{(\mathcal{E} - \mathcal{E}_{\mu}^0)} \right] \equiv \sum_{\mu} \frac{1}{m_{\mu}^*(\mathcal{E})}$$

$$g^*(\mathcal{E})\sigma_z = \frac{4m}{i} \sum_{\mu} \left[\frac{\pi_{j\mu}^x \pi_{\mu j}^y}{(\mathcal{E} - \mathcal{E}_{\mu}^0)} \right] \equiv \sum_{\mu} g_{\mu}^*(\mathcal{E})\sigma_z.$$

In the absence of magnetic field, (A3) gives the cubic equation of Kane, Eq. (2). The eigenvalues of Eq. (A3) for $k_H=0$ are

$$\mathcal{E} = \left(n + \frac{1}{2}\right) \frac{\hbar e H}{m^*(\mathcal{E})c} \pm \frac{1}{2} g^*(\mathcal{E})\beta H,$$

or,

$$\mathcal{E} = \left(n + \frac{1}{2}\right) \frac{\hbar e H}{c} \sum_{\mu} \frac{1}{m_{\mu}^*(\mathcal{E}_j^0)} \left(\frac{\mathcal{E}_j^0 - \mathcal{E}_{\mu}^0}{\mathcal{E} - \mathcal{E}_{\mu}^0} \right) \pm \frac{1}{2} \beta H \sum_{\mu} g_{\mu}^*(\mathcal{E}_j^0) \left(\frac{\mathcal{E}_j^0 - \mathcal{E}_{\mu}^0}{\mathcal{E} - \mathcal{E}_{\mu}^0} \right). \quad (\text{A4})$$

In the limit where the energy of excitation above the j th band edge is small compared to the band gaps, the sums become the values of $1/m^*$ and g^* at the bottom of the j th band. $m^*(\mathcal{E})$ and $g^*(\mathcal{E})$ must be interpreted with caution. $m^*(\mathcal{E})$ is not, for example, the mass value measured in a cyclotron resonance experiment performed on carriers at an energy \mathcal{E} in the band.

Fine Structure and Magneto-Optic Effects in the Exciton Spectrum of Cadmium Sulfide*

J. J. HOPFIELD

Bell Telephone Laboratories, Murray Hill, New Jersey, and Laboratoire de Physique, École Normale Supérieure, Paris, France

AND

D. G. THOMAS

Bell Telephone Laboratories, Murray Hill, New Jersey

(Received November 15, 1960)

The valence band of cadmium sulfide is split by spin-orbit and crystal field effects into three nearly degenerate bands at $\mathbf{k}=0$. The magneto-optic absorption spectrum of direct excitons formed from the top valence band and the conduction band has been studied in detail. Most of the experiments reported have been performed in light polarized parallel to the hexagonal axis. In this geometry, the exciton series consists of weak lines amenable to magneto-optic experiments. When the magnetic field and the wave vector of the light are perpendicular to each other and to the hexagonal axis, the reversal of the magnetic field produces large changes in the absorption spectrum. This effect can be quantitatively understood as an interference effect between allowed exciton transitions (optical matrix elements independent of the wave vector of the light) and forbidden exciton transitions (optical matrix elements proportional to the wave vector of the light). It is shown that in CdS the forbidden processes having a principal quantum number 2 are somewhat stronger than allowed processes of the same quantum number. By using group theory and the effective-mass approximation, the electron and hole anisotropic g values and masses are determined from an analysis of the exciton spectrum. The electron mass, $0.20_5 m$ (almost isotropic), determined in this analysis is compatible with the assumption that the $\mathbf{k}=0$ conduction band valley is the lowest conduction band valley. The hole masses for the top valence band are $m_{h1} = 0.7 m$ and $m_{h11} \approx 5 m$. An experimental upper limit on the slope of the conduction band at $\mathbf{k}=0$ is obtained.

I. INTRODUCTION

IN a previous paper¹ the reflection spectrum of CdS at low temperatures was described and led to the identification of three separate intrinsic exciton series A , B , and C . Series A , occurring at lowest photon energies, was strongly active only for light polarized with its E vector perpendicular to the hexagonal c axis of the crystal (hereafter denoted $E \perp c$). Series B and C were active for both modes of polarization of the light.

* This work was supported in part by the Air Research and Development Command, United States Air Force.

† Now at the Ecole Normale Supérieure, Laboratoire de Physique, Paris.

¹ D. G. Thomas and J. J. Hopfield, Phys. Rev. **116**, 573 (1959).

These results were explained in terms of excitons being formed from an electron in the conduction band and a hole from each one of the three valence bands. The three bands result from a complete lifting of the degeneracy of the three p -like bands at $\mathbf{k}=0$ (the center of the Brillouin zone), under the influence of crystal field and spin-orbit coupling effects. The symmetry of the top valence band was shown to be Γ_9 and the others Γ_7 . The $n=1$ quantum states of the excitons were readily detected at 77°K but the weaker $n=2$ states only became apparent at 4.2°K. The identification of the intrinsic exciton states made possible interpretation of some absorption results of other workers.

In general, reflection peaks are broad and do not lend themselves to Zeeman effect measurements. In addition the allowed intrinsic exciton transitions have considerable oscillator strength which makes their observation in absorption difficult unless extremely thin crystals are used; (there are numerous weaker "impurity exciton" transitions but at present the precise origin of these lines is not known). Fortunately, the allowed strong transitions of exciton series A in CdS are not active in $E\parallel c$ light and certain weak "forbidden" transitions may be observed as sharp lines in absorption using this polarization. This paper is largely devoted to a study of these lines with the object of deriving information concerning excitons and the band structure of CdS.

In Sec. II, the experimental methods are described. Sec. III contains the general experimental results and qualitative description of their interpretation. In Sec. IV the quantitative aspects of the energy level structure and line strengths are derived in effective mass approximation. These results are applied in Sec. V to obtain the anisotropic masses and g values of electrons and holes from a fit to the observed magneto-optic spectrum. The theoretical explanation of the alteration of certain magneto-optic absorption spectra with the reversal of the magnetic field (in linearly polarized light) is given in Sec. VI. Direct experimental verification of strong forbidden exciton transitions is obtained. The effect of the finite-slope band crossing and other minor perturbations are discussed in Sec. VII.

II. EXPERIMENTAL

A Bausch and Lomb spectrograph was used with a 4-in. \times 4-in. grating having 55 000 lines/inch. A dispersion of 2 Å/mm in the first order was obtained. The slit width used was 50 μ . The detector was a photographic plate, useful both because of its sensitivity and because it allowed the detection of strain in the crystals since this appeared as an alteration in the frequency of the absorption lines from one part of the crystal to another. The crystal was glued at one end over an aperture in a molybdenum plate; sometimes the crystals were only large enough to cover a circular aperture

TABLE I. A summary of the data for some of the absorption lines seen in light polarized perpendicular to the hexagonal c axis. $E\perp c$; temperature, 1.6°K.

Line	Position		(Approx. apparent width) $\times 10^3$ (ev)	Crystal
	(Å)	(ev)		
I_1	4888.6	2.5359	0.3	GEB3
I_2	4868.7	2.5463	0.5	GEA1
I_3	4859.0	2.5513	0.3	GEA1
$A, n=1(1S_T)$	4854.5	2.5537	3.5	GEA1
I_4	4837.7	2.5626	1.7	GEB3
$B, n=1$	4826.4	2.5686	3.5	GEA1
$A, n=2$	4812.9	2.5758	3	GEA1

0.025 in. in diameter. Crystals showed remarkable differences in the sharpness of the lines; in particular in some crystals 5–10 μ thick at 1.6°K the P_z component of the $n=2$ line (see below) could not be seen, while in "good" crystals it was clearly visible. In these good crystals the $n=2, 3,$ and 4 lines become markedly sharper on cooling from 4.2 to 1.6°K, and the properties of such crystals are reported here. The crystals were immersed in the refrigerant and the Dewar vessel tip could be inserted between the pole pieces of a magnet $\frac{5}{8}$ in. apart.

III. RESULTS

$E\perp c$

In Table I are listed some of the impurity lines and the intrinsic exciton lines seen in absorption for light polarized with $E\perp c$. The impurity lines cited (I_1 to I_4) are certainly not the only such lines which occur but they are quite prominent. These lines vary in intensity from one crystal to another; thus crystal GED7 (thickness, $t=6 \mu$) which gave very "good" exciton lines had no detectable impurity lines; however, GED8 ($t=12 \mu$), also a very good crystal, did show the impurity effects and it is not considered likely that the difference in t is alone sufficient to account for this. Crystal GEB3, somewhat thinner than GED7, which was of rather inferior quality did show the impurity lines. I_1 is a weak line; I_2 is much stronger and in one crystal it has been observed as a well defined triplet with a separation between each member of the triplet of about 0.00025 ev. I_1 and I_2 correspond to the emission lines labeled "doublet" and "singlet," respectively, in the previous work¹; at present no great weight is put on the multiplicity of I_1 in emission as the absorption lines may show differing multiplicity from one crystal to another. At photon energies slightly above I_2 there are often many weak lines and then a fairly strong line I_3 just below the $n=1$ state of exciton A . I_4 occurs in the intrinsic exciton region; however, as it is present in some crystals but not in others, it is considered to be an impurity effect. It is perhaps analogous to I_2 being an impurity exciton derived from exciton B rather than exciton A . It is remarkable for being broad whereas other impurity lines are quite sharp; this broadening may arise from a very short lifetime as a vibrational transition may change the state into the corresponding state derived from exciton A . Wheeler² has reported similar impurity lines some of which lie near those quoted here, and has described the effect of a magnetic field on the spectra.

All the intrinsic exciton absorptions active in $E\perp c$ appear broad in the crystals examined; since the light is totally obscured at and near the absorption peaks the apparent width is not necessarily equal to the half width of the line. The midpoints of the lines are quoted

² R. G. Wheeler, Phys. Rev. Letters **2**, 463 (1959); R. G. Wheeler and J. O. Dimmock, Phys. Rev. Letters **3**, 372 (1959).

in Table I; however, because of the linewidth these positions are not very precise, and in addition since there is a sizable reflection anomaly at the $n=1$ positions it is not to be expected that the absorption midpoints precisely correspond to the resonant frequencies of the transitions.

At 20°K the impurity lines are slightly less sharp than at 1.6°K. In common with lines A_F and A_L (see below) they move about 1 Å to longer wavelengths as the temperature is raised from 1.6 to 20°K which indicates that all the lines originate from the same band extrema. It may be added that at 20°K the reflection anomalies previously reported¹ at the $n=2$ positions of excitons A and B have practically vanished as a result of thermal broadening.

$E\parallel c$

For light polarized with $E\parallel c$ few impurity lines have been seen in the crystals used for this work. One such line is I_4 listed in Table II; as for $E\perp c$ this line is broad. Thin crystals reveal broad allowed transitions to the $n=1$ and $n=2$ states of exciton B .

Of greater interest are a number of comparatively weak and sharp lines to levels derived from exciton A . These lines are always present and represent intrinsic effects, although the $n=2, 3, 4$ states are broader in some crystals than in others. In order of increasing photon energy the lines at 1.6°K occur as follows (see Table II).

$A_F(1\Gamma_6)$

This is a weak sharp line seen most readily in crystals of thickness 5 μ or more. It is a forbidden transition occurring because of the finite momentum of the photon which induces the transition. It represents the Γ_6 $n=1$ state of exciton A in which the spins of the electron and hole are parallel; if the midpoint of the strong absorption seen for $E\perp c$ is taken as the resonant frequency for the Γ_5 state of exciton A , then the Γ_6 state lies 0.0013 ev below the Γ_5 state (in which the spins are antiparallel). Uncertainty in the position of

Γ_5 is not likely to account for such a large separation. This separation may arise partly from a configurational mixing of the Γ_5 states of excitons A and B , and partly from the long-range Coulomb terms which will be much more important for the strong Γ_5 than for the weak Γ_6 states; simple spin-spin effects are probably much too small to account for the observed energy difference. The twofold degeneracy of the Γ_6 state is lifted by a magnetic field along the c axis ($H\parallel c$); a linear Zeeman effect results giving a g value of 2.93 in good agreement with a value of 2.93 ± 0.03 as reported by Wheeler² for the same line. (A fuller discussion of some of the points mentioned in this paragraph is given below and also by Hopfield.³)

It is interesting (and unfortunate) that no forbidden transition can be seen corresponding to the Γ_{5T} state. Group theoretic analysis along the lines of Sec. IV-C indicates that this Γ_{5T} line is more highly forbidden (actually third forbidden) than the $1\Gamma_6$ line, and this probably accounts for its nonobservance since it would be expected to be correspondingly weaker than the already weak $1\Gamma_6$ line.

$A_L(1S_L)$

This line lies approximately 0.0008 ev above the center point of the $E\perp c$ strong absorption line. It is remarkable for the fact that as the crystal is rotated about an axis perpendicular to the c axis its optical strength increases very rapidly. This is seen as an increase in the absorption coefficient, and when this is sufficiently large to completely obscure the light the apparent width of the line increases. The effects are clearly visible for rotations of less than 10°, over which range the other lines in the spectrum show no appreciable change. This behavior is precisely that to be expected for a "longitudinal" exciton⁴ in a uniaxial crystal, and in fact A_L is the longitudinal exciton derived from the strong allowed "transverse" Γ_5 transition. An estimate of the expected transverse-longitudinal energy difference may be made from the relations of reference 4, and from an estimate of the hypothetical value of the refractive index of CdS for $E\perp c$, at the wavelength of A_L in the absence of exciton A , together with a knowledge of the oscillator strength of A .¹ A value of 0.0018 ev is obtained; in view of the many uncertain quantities, not least of which is the precise determination of the resonant energy of the transverse exciton, this is considered to be in reasonable agreement with the experimental value of 0.0008 ev quoted above.

The coupling to the Γ_5 exciton under conditions of slight misalignment takes place because a small component of the E vector may be resolved in a direction perpendicular to c and so interacts with the allowed Γ_5

TABLE II. A summary of the data for some of the absorption lines seen in light polarized parallel to the hexagonal c axis. $E\parallel c$; temperature, 1.6°K.

Line	Position		(Approx. apparent width) $\times 10^3$ (ev)	Crystal*
	(Å)	(ev)		
$A_F(1\Gamma_6)$	4857.0	2.5524	0.1	GED7
$A_L(1S_L)$	4852.9	2.55455		
I_4	4837.7	2.5626	1.7	GEB3
$B, n=1$	4826.1	2.5687	4.3	GEA1
$A, n=2$	4814.21	2.57508	0.1	GED7
	4812.96	2.57575	0.4	GED7
$A, n=3$	4805.46	2.57977	0.5	GED7
$A, n=4$	4803.28	2.58094	0.3	GED7
$B, n=2$	4784.9	2.59085	3.5	GEA1

* Crystal thickness t : GEA1 $\sim 1 \mu$, GED7 $\sim 6 \mu$, and GEB3 $\sim 2.9 \mu$.

³ J. J. Hopfield, J. Phys. Chem. Solids **15**, 97 (1960).

⁴ J. J. Hopfield and D. G. Thomas, J. Phys. Chem. Solids **12**, 276 (1960).

transition. The direction of propagation of the exciton, which is the same as that of the photon, is now almost identical with the direction of the polarization vector of the exciton, and this results in a "longitudinal" exciton. In general the wave is not pure longitudinal and becomes less so as the misalignment is increased; it is expected therefore, that as the crystal is rotated the "longitudinal" line should converge on the transverse line. This effect is not observed since the rapid broadening of the line with rotation as observed in crystals only a few microns thick prevents the precise location of the resonant frequency. One further complication is that the line does appear weakly when the light is traveling precisely perpendicular to the c axis; this is to be ascribed to the fact that the photon has a finite momentum so that the transitions are not exactly at $\mathbf{k}=0$. In this orientation α , the absorption coefficient, at the peak A_L has a value of the order of 500 cm^{-1} .

The existence of the longitudinal-transverse energy difference which is large compared to any expected Zeeman splitting, results in the quenching of the Zeeman effect for the Γ_6 line.⁴ For the Γ_6 line the longitudinal-transverse effects are negligible as the oscillator strength is so small, and a Zeeman effect is observed.

A, $n=2$

In zero magnetic field this state has two components, a strong line near 2.57575 eV and a much weaker one at 2.57508 eV. This is illustrated in Fig. 1(c) which shows a microphotometer trace of a plate (Kodak SAI) taken with crystal GED8 of thickness $12\ \mu$. The

application of a magnetic field produces a variety of effects on these lines depending on the geometry of the system; these will now be described.

(a) $H\parallel c, q\perp H$ (\mathbf{q} is the wave vector of the exciting photon). Figure 2 shows that in this geometry at 31 000 gauss a total of seven lines can be seen. The weak line denoted by P_z undergoes a quadratic diamagnetic shift to higher energies and splits at higher fields giving a g value of 0.62 ± 0.06 . The strength of the line is not materially affected by the field. The remaining lines are derived from the strong line and have the approximate strengths shown in Fig. 2 (see also Table IV). Experiments were performed at 31 000 gauss in which the crystal was rotated with respect to the light beam about an axis perpendicular to c . As the misalignment increased the line marked S_L rapidly increased in strength; for the correct alignment S_L practically vanished and Fig. 2 represents the results for a misalignment of about 5° . The line (S_T, P_x-iP_y) also increased with angle but the effect was not as large as for S_L and the line did not go to zero strength at zero angle.

Clearly for an $n=2$ state there can be both S and P states. A magnetic field is not expected to mix S and P states but will mix the P states with orbital angular momentum directed at right angles to the field; in addition it is expected to mix longitudinal and transverse S states if the zero-field separation between them is small. In the long-wavelength limit and for perfect alignment, group theory indicates that a P state (Γ_1), which will split in a magnetic field by combining with a Γ_2 state, is the only allowed transition for this mode

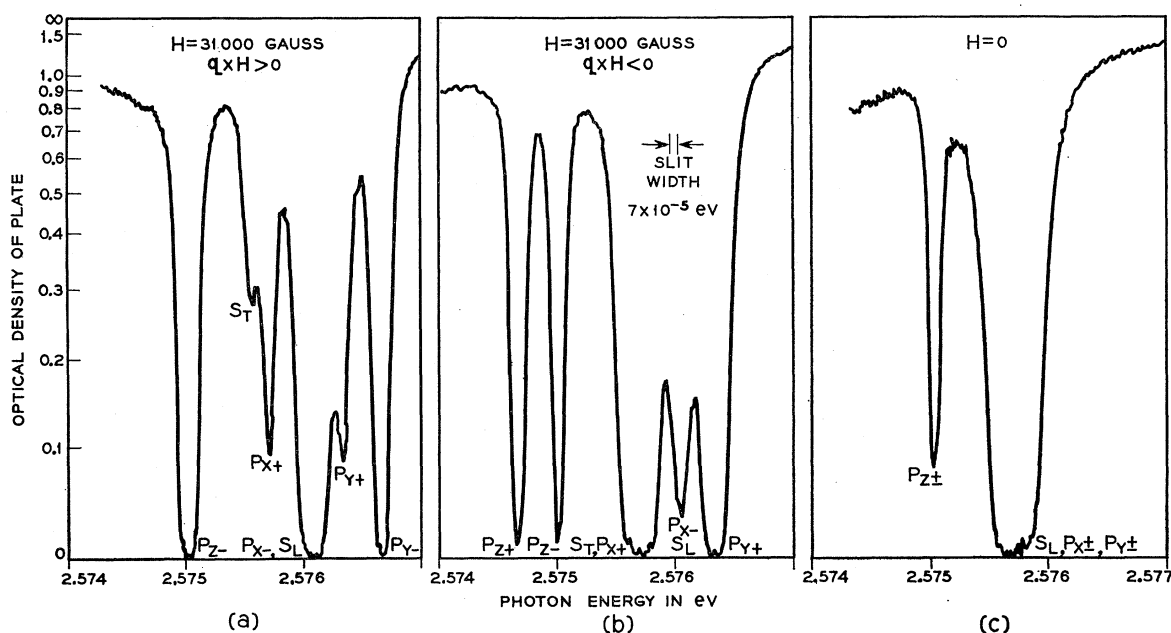


FIG. 1. Microphotometer trace of Zeeman effects of the $n=2$ exciton states in CdS crystal GED8 at 1.6°K . $c\perp H, H\parallel x, q\perp H$, and $q\perp c$. \mathbf{q} is here the wave vector of the exciting photon.

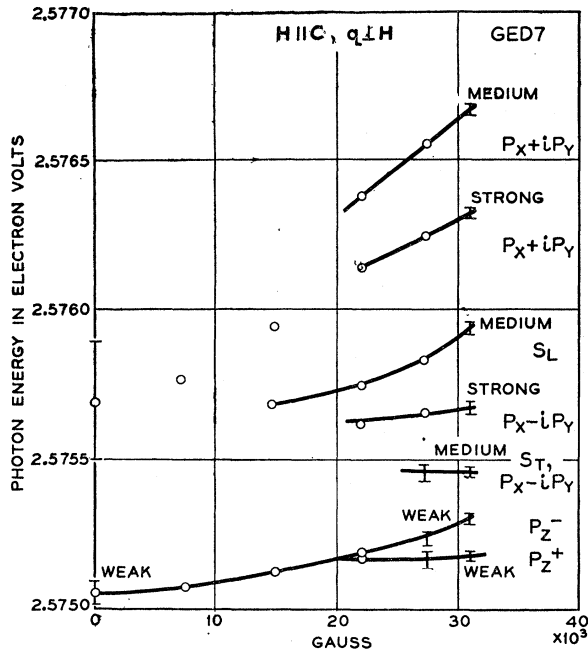


FIG. 2. The Zeeman effect at 1.6°K for $H\parallel c$. At $H=0$ the limits indicate the apparent line widths, otherwise they indicate the approximate uncertainty in the line positions.

of polarization; (this transition falls into Elliott's⁵ "forbidden" class; it occurs because the exciton includes states from the valence and conduction bands which are not at $\mathbf{k}=0$; this mechanism does not allow transitions to S states). It is evident from experiment that other lines can occur for a variety of reasons. The rotation experiment shows that S_L is a longitudinal exciton which must be derived from the S state seen for light with $E\perp c$. Since $(S_T, P_x - iP_y)$ also increases with angle it presumably contains the transverse S state, although as it does not vanish at zero angle it must contain another state. This state must be a P state which may be paired with the highest energy state of this group. The remaining weak line must be the P state with zero angular momentum about the c axis and is denoted by P_z ; it is split by spin effects and does not mix with any other states in this geometry.

(b) $H\perp c, q\parallel H$ (or $-q\parallel H$) (for definiteness we assume $H\parallel x$). Figure 3 gives the results for this geometry in which the light is traveling parallel to the magnetic field. (This condition was achieved by using a crystal holder which acted as a double mirror each reflection turning the light beam through 90°.) It is now expected that P_y and P_z states will be mixed by the field and in accord with this P_z is moved to lower energies and increases in strength as the field is increased. The greater intensity results from mixing with the stronger P_y states. The splitting of the P_z state is now greater than for $H\parallel c$; this is because the spin magnetic moment

of the exciton arises from the difference of the electron and hole spin moments for $H\parallel c$, whereas for $H\perp c$ the hole moment does not interact with H and the splitting arises from the electron spin moment alone. (The curious intensity ratios of this spin doublet will be discussed in Sec. VI.) The P_y states must be the top-lying pair which move rapidly to higher energies with increasing field. The P_x states suffering only a diamagnetic shift and a spin splitting are as shown. Although rotational experiments were not performed for this particular geometry, other experiments with $H\perp c$ showed that the transverse and longitudinal S states were in the positions indicated. The S_L state is not separated from a P_x state while the S_T state is now seen alone (for $H\parallel c$ the opposite is true).

(c) $H\perp c, q\perp H, q\perp c$. In this geometry there occurs a remarkable effect shown in Figs. 1(a) and 1(b),⁶ which demonstrates that at 31 000 gauss two different spectra occur for the two directions of H . This effect has been observed for several crystals. It has been shown that if the crystal is rotated 180° about the c axis no

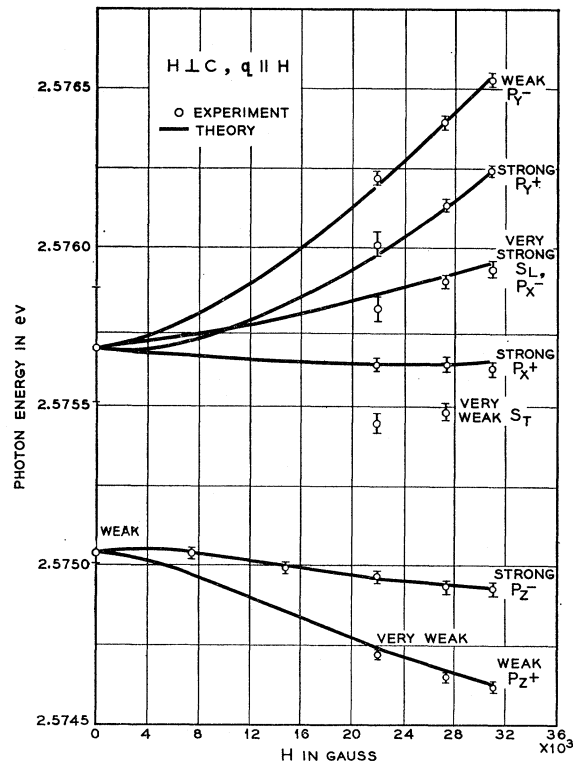


FIG. 3. The Zeeman effect at 1.6°K for $H\perp c$ and $q\parallel H$, i.e., the light is here traveling parallel to the magnetic field. In this diagram the lines represent theory (see Sec. V); the mass values A have been used and the following values are employed: rydberg=0.027 eV, $\gamma=0.222$, $g_{e\perp}=1.73$, and $g_l=8.3$. As before, the limits on the experimental points at $H=0$ indicate the apparent linewidth; otherwise they indicate the approximate uncertainty in the line positions.

⁵ R. J. Elliott, Phys. Rev. **108**, 1384 (1957).

⁶ J. J. Hopfield and D. G. Thomas, Phys. Rev. Letters **4**, 357 (1960).

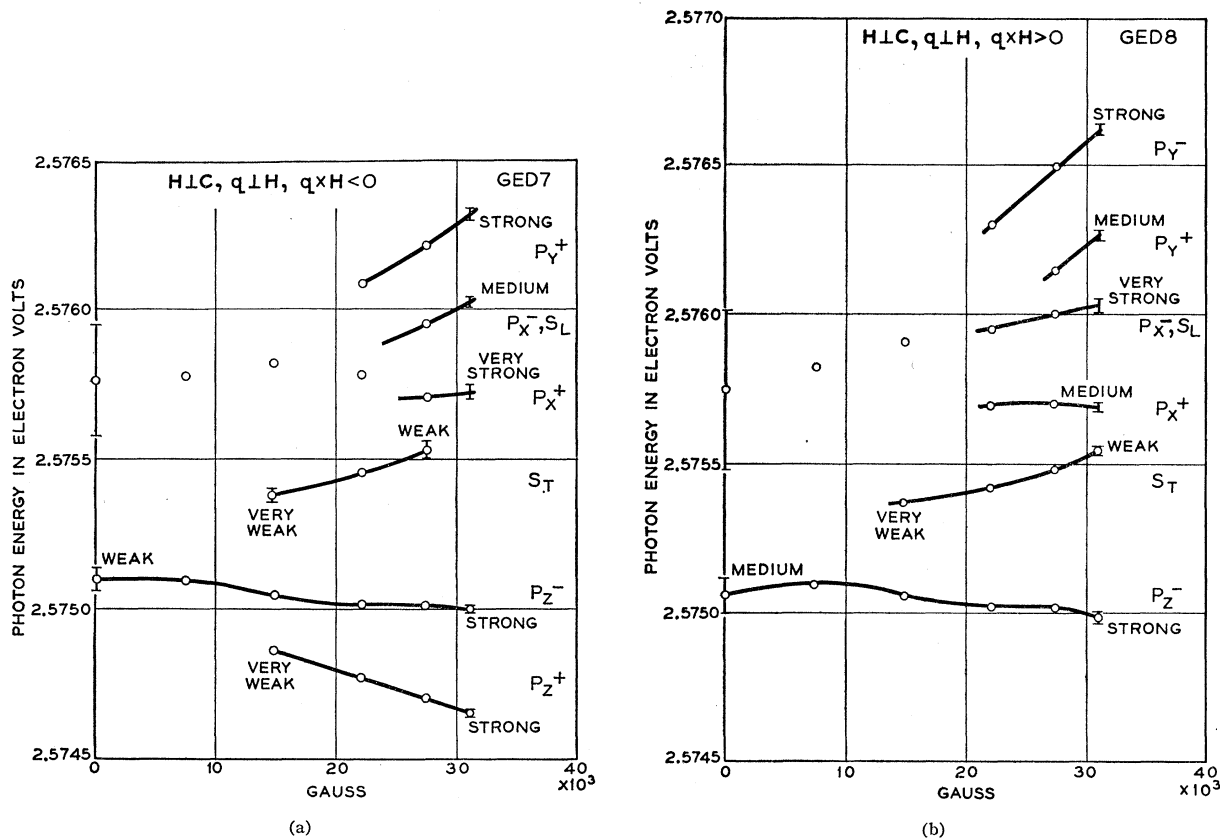


FIG. 4. The Zeeman effect at 1.6°K for $H \perp c$ and $q \perp H$ for the two directions of H . (a) is termed the "doublet" spectrum, and (b) the "singlet" spectrum.

change results, but that a rotation of 180° about q changes one type of spectra into the other. Figures 4(a) and 4(b) show how the two spectra vary with magnetic field. In Fig. 4(a), P_z occurs as a doublet and so for convenience this spectra may be termed "doublet" while Fig. 4(b) may be called the "singlet" spectra. Rotation experiments indicated that the S states occur as shown. It is seen that within experimental uncertainty (about $\pm 2 \times 10^{-5}$ eV for a particular crystal) all of the lines which occur for $q \parallel H$ occur in one or both of the spectra for $q \perp H$ at the same energy positions. The relative strengths of the lines are, however, quite different for the three spectra.

$n=3, 4$ and Higher States

In zero magnetic field $A, n=3$ and $A, n=4$ can be seen for $E \parallel c$. However, beyond the calculated series limit the absorption decreases (until $B, n=2$ is approached) which is surprising and presumably arises because the "wrong" mode of polarization is being used (see also Sec. IV-C). In a magnetic field the states split and undergo large diamagnetic shifts. Figure 5 shows the behavior for $H \parallel c$. The $n=3$ state splits predominantly into two components giving a g value

of 10.8. Some of the $n=4$ states probably overlap the $n=3$ states and presumably also the $n=5$, etc., states. For $H \perp c$ complex splitting is seen and the spectra for the two directions of H are different. It is clear that the Coulomb energies are comparable to the magnetic energies and the exciton spectrum must merge into one better described in terms of Landau levels. In fact at high fields rather broad absorption maxima can be discerned in the continuum region. Some of the lines increase in strength as the crystal is rotated about an axis perpendicular to c and they have been marked S .

Reflection Anomalies

It has been previously mentioned¹ that the reflection peak of exciton B showed unexpected structure for $E \perp c$. In other crystals structure is seen for exciton A as well as B and Fig. 6 shows microphotometer traces of reflection spectra showing this effect. For $E \parallel c$ light exciton B does not show structure. Such structure is unlikely to occur as a result of impurity effects; it probably is not apparent in some crystals because of imperfect structure in these crystals. The origin of such structure is not at present definitely known, although a possible origin is discussed below.

IV. THEORY

A. Band Symmetry and Energy Band Structure

From previous work,¹ it appears almost certain that the direct band gap in CdS lies either at the point Γ or along the line Γ -A, which has the same symmetry as the point Γ . The conduction band is believed to be of symmetry Γ_7 , and the top valence band of symmetry Γ_9 .⁷ The bands are twofold degenerate along the line Γ -A, but can split in the presence of spin-orbit coupling into nondegenerate bands^{8,9} away from this line. The conduction band is allowed from symmetry considerations to split so that the energy is proportional to the component of \mathbf{k} perpendicular to the line Γ -A (i.e., perpendicular to the c axis). The valence band can split only quadratically. We have made a theoretical estimate of these splittings, and have come to the conclusion that they should be very small. All the experimental results seem susceptible to simple interpretation without the necessity of an observable "spin" splitting of the conduction or valence bands, justifying in a sense our neglect of the spin splitting (see also Sec. VII).

The possibility of two equivalent "direct band gaps" along the line Γ -A cannot be totally ignored. We will discuss all the exciton states as if there were one con-

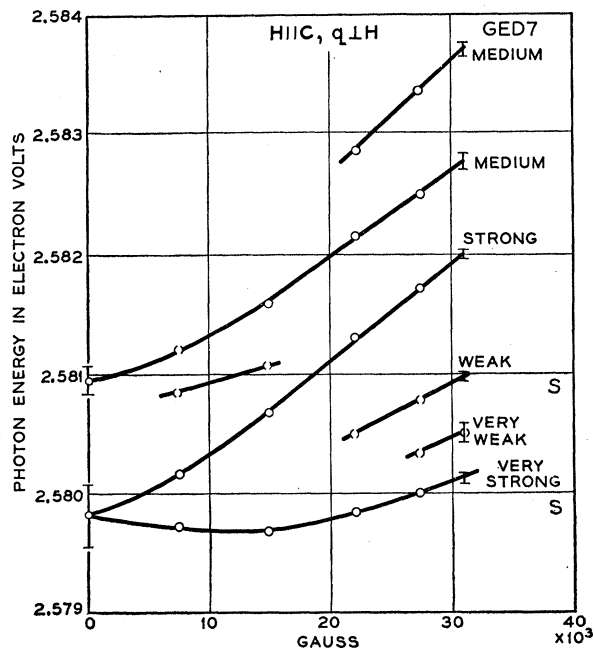


FIG. 5. The Zeeman effect of the higher exciton states at 1.6°K for $c||H$. The lines marked S increase in strength as the crystal is rotated about an axis perpendicular to c .

⁷ J. L. Birman, Phys. Rev. Letters 2, 157 (1959).

⁸ R. C. Casella, Phys. Rev. 114, 1514 (1959).

⁹ M. Balkanski and J. des Cloizeaux, J. Phys. Chem. Solids (to be published).

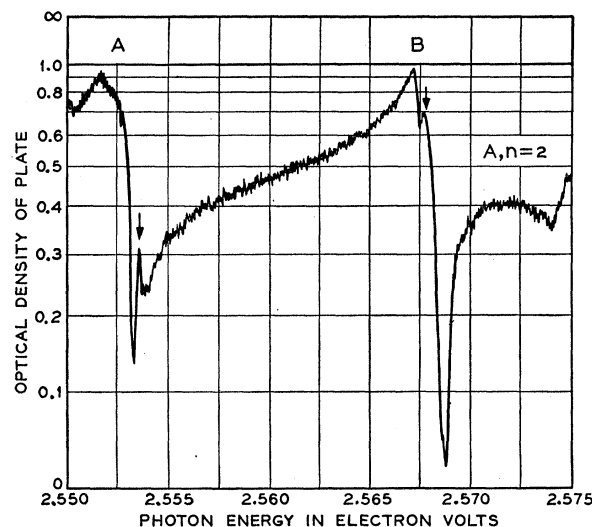


FIG. 6. Microphotometer trace of reflection spectrum of CdS crystal GM3 at 4.2°K, for light with $E \perp c$. The anomalous structure referred to in the text is indicated by the arrows.

duction band minimum and one valence band maximum at $\mathbf{k}=0$. The existence of two band minima would double the number of possible exciton states. For weakly bound excitons there would be an additional quantum number which would specify the valley of the exciton, and all excitons would necessarily have a twofold (or greater) degeneracy. For tightly bound excitons, mixing between the valleys could occur, giving rise, for example, to a split exciton ground state. The situation is completely analogous to the donor wave functions in silicon and germanium. No observable effects due to the existence of two minima (if indeed there are two minima) are expected to be capable of observation for the excited exciton states.

"The reflection anomalies" seen in some cases for the ground-state exciton could be caused by a two valley band structure. Unfortunately the analysis of the electron and hole g values even for the ground state, turns out to be essentially independent of whether there are one or two valleys. Only the estimates of the relative strengths of different allowed and forbidden exciton transitions is sensitive to the possibility of multiple valleys. For this purpose, a single valley at $\mathbf{k}=0$ has been assumed.

B. The Exciton States in Effective Mass Approximation

The following symbols will prove useful: $m_{e\perp}$ ($m_{h\perp}$) = electron (hole) effective mass perpendicular to the c axis; $m_{e\parallel}$ ($m_{h\parallel}$) = electron (hole) effective mass parallel to the c axis; m = free electron mass; x_e, y_e, z_e (x_h, y_h, z_h) are electron (hole) coordinates; ϵ_{\perp} (ϵ_{\parallel}) is the low-frequency (clamped) dielectric constant perpendicular (parallel) to the c axis. The z

direction will be chosen as the direction of the hexagonal axis.

The Schrödinger equation¹⁰ which must be solved for the exciton energy levels is

$$\left\{ -\frac{\hbar^2}{2m_{e\perp}} \left(\frac{\partial^2}{\partial x_e^2} + \frac{\partial^2}{\partial y_e^2} \right) - \frac{\hbar^2}{2m_{e\parallel}} \left(\frac{\partial^2}{\partial z_e^2} \right) - \frac{\hbar^2}{2m_{h\perp}} \left(\frac{\partial^2}{\partial x_h^2} + \frac{\partial^2}{\partial y_h^2} \right) - \frac{\hbar^2}{2m_{h\parallel}} \left(\frac{\partial^2}{\partial z_h^2} \right) - e^2 [\epsilon_{\perp} \epsilon_{\parallel} (x_e - x_h)^2 + \epsilon_{\perp} \epsilon_{\parallel} (y_e - y_h)^2 + \epsilon_{\perp}^2 (z_e - z_h)^2]^{-\frac{1}{2}} \right\} \psi = E\psi. \quad (1)$$

In (1), the zero of energy has been chosen as the band gap. If the center-of-mass coordinate is removed from (1) and the center-of-mass momentum set equal to zero, one obtains the usual reduced mass equation (2)

$$\left\{ -\frac{\hbar^2}{2\mu_0} \nabla^2 - \frac{\hbar^2}{2\mu_0} \left(\frac{2\gamma}{3} \right) \left(\frac{1}{2} \frac{\partial^2}{\partial x^2} + \frac{1}{2} \frac{\partial^2}{\partial y^2} + \frac{\partial^2}{\partial z^2} \right) - \frac{e^2}{\epsilon_0 r} \right\} \psi = E\psi \dots, \quad (2)$$

where

$$x = x_e - x_h, \quad y = y_e - y_h, \quad z = \left(\frac{\epsilon_{\perp}}{\epsilon_{\parallel}} \right)^{\frac{1}{2}} (z_e - z_h),$$

$$\epsilon_0 = (\epsilon_{\perp} \epsilon_{\parallel})^{\frac{1}{2}}, \quad \frac{1}{\mu_1} = \frac{1}{m_{e\perp}} + \frac{1}{m_{h\perp}}, \quad \frac{1}{\mu_{\parallel}} = \frac{1}{m_{e\parallel}} + \frac{1}{m_{h\parallel}},$$

$$\frac{1}{\mu_0} = \frac{1}{\mu_0} + \frac{2}{3} \frac{1}{\mu_1} + \frac{1}{3} \frac{1}{\mu_{\parallel}} \frac{\epsilon_{\perp}}{\epsilon_{\parallel}}, \quad \gamma = \mu_0 \left(\frac{1}{\mu_1} - \frac{1}{\mu_{\parallel}} \frac{\epsilon_{\perp}}{\epsilon_{\parallel}} \right).$$

The energy levels are thus determined by a mean reduced mass μ_0 , a mean dielectric constant ϵ_0 , and a single anisotropy parameter γ .

The effective-mass approximation is expected to be an excellent approximation for the states $n=2$ and above, which have binding energies 0.007 eV and less, and radii 100 Å and greater. Only for the $n=1$ state ($E_B \approx 0.028$ eV, radius ~ 25 – 30 Å) does one expect to find noticeable deviations from the effective mass approximation. For the $n=1$ state, the binding energy is comparable to the energy of a longitudinal optical phonon (0.039 eV) and the use of the low-frequency dielectric constant is no longer correct.¹¹ In addition, the radius is only ~ 10 lattice spacings, and central cell corrections to the wave function may become important.

For the case at hand, experimental evidence shows that the anisotropy is small, so that the state energies need be computed only to lowest order in the anisotropy.

The problem is formally identical to that of the donor states in silicon or germanium.¹² The state energies in units of the mean rydberg, $e^4 \mu_0 / 2 \hbar^2 \epsilon_0^2$, are

$$\begin{aligned} 1S: & -1, & 3D_0^*: & -\frac{1}{9} \left(1 + \frac{4}{21} \gamma \right), \\ 2S: & -\frac{1}{4}, & 3D_{\pm 1}: & -\frac{1}{9} \left(1 + \frac{2}{21} \gamma \right), \\ 2P_0: & -\frac{1}{4} \left(1 + \frac{4}{15} \gamma \right), & 3D_{\pm 2}: & -\frac{1}{9} \left(1 - \frac{4}{21} \gamma \right), \\ 2P_{\pm 1}: & -\frac{1}{4} \left(1 - \frac{2}{15} \gamma \right), & 4S^*: & -\frac{1}{16}, \\ 3S^*: & -\frac{1}{9}, & & \text{etc.} \\ 3P_0: & -\frac{1}{9} \left(1 + \frac{4}{15} \gamma \right), & & \\ 3P_{\pm 1}: & -\frac{1}{9} \left(1 - \frac{2}{15} \gamma \right), & & \end{aligned}$$

The subscripts 0, ± 1 , etc., refer to the number of units of orbital angular momentum around the c axis (z direction).

The states marked with an asterisk in the preceding list have energies which should be computed using degenerate perturbation theory. For example, the perturbation mixes the states $3S$ and $3D_0$. Calculation shows, however, that these off diagonal matrix elements of the anisotropy perturbation produce changes so small in the calculated energies that for γ near 0.2 the effects of these terms are only of the order of magnitude of γ^2 correction terms. The effect of these cross terms has therefore been omitted.

The first order perturbation theory energies are poor estimates of the actual binding energies at and above $n=5$, for the separation between hydrogenic levels differing by 1 in their main quantum number becomes comparable to the first order energy shifts.

C. Group-Theoretic Analysis of the Exciton States; Line Strengths

One can directly calculate, by the methods of reference 3, the symmetry of the excitons including electron and hole spins. There is much excess degeneracy present when the effective-mass theory is valid, and such group-theoretic calculations are essential to determine which states are being observed. One finds for the

¹⁰ G. Dresselhaus, Phys. Rev. **106**, 76 (1957).

¹¹ H. Haken, J. Phys. Chem. Solids **8**, 166 (1959).

¹² W. Kohn, in *Solid-State Physics*, edited by F. Seitz and D. Turnbull (Academic Press, Inc. New York, 1957), Vol. 5, pp. 257–295.

conduction and valence bands already discussed, the decomposition

$$\begin{aligned} 1S, 2S, 3S &\rightarrow \Gamma_5 + \Gamma_6, \\ 2P_0, 3P_0 &\rightarrow \Gamma_5 + \Gamma_6, \\ 2P_{\pm 1}, 3P_{\pm 1}, 3D_{\pm 1} &\rightarrow \Gamma_1 + \Gamma_2 + \Gamma_3 + \Gamma_4 + \Gamma_5 + \Gamma_6, \\ 3D_{\pm 2} &\rightarrow \Gamma_1 + \Gamma_2 + \Gamma_3 + \Gamma_4 + \Gamma_5 + \Gamma_6. \end{aligned}$$

The existence of a $2P_{\pm 1}$ state of symmetry Γ_1 (and therefore an allowed exciton transition in light polarized parallel to the c axis) was one of the main reasons for starting our experimental study. This line was expected to have a suitable strength for easy study in available crystals, to have an interesting g value, and not to be obscured by stronger less interesting exciton lines.

The selection rules for light of infinite wavelength allow transitions only to excitons of symmetry Γ_1 for light polarized parallel to the hexagonal axis. Light of a finite wavelength, however, interacts with excitons of nonzero wave vector and can permit other exciton transitions. The wave vector \mathbf{q} of the light is so small compared to a reciprocal lattice vector that the exciton states, from the point of view of their energy, may be considered to have zero wave vector. It therefore becomes convenient to describe the exciton states at $\mathbf{k}=0$, and to regard the finite wave vector of the light as a perturbation which allows an additional form of optical coupling. Let the wave vector of the light be in the y direction (perpendicular to the hexagonal axis). Then, in addition to the Γ_1 allowed excitons, it becomes possible to observe excitons of symmetry Γ_{5y} . These transitions will have optical matrix elements proportional to the wave vector \mathbf{q}_y of the light and will be called first forbidden transitions. All other exciton transitions have optical matrix elements proportional to higher powers of the wave vector of the light, and can by and large be ignored.

Elliott⁵ has considered in some detail the calculation of oscillator strengths for allowed exciton transitions in the cases in which (1) the band symmetry is such that optical transitions are allowed at the direct band gap and (2) the band symmetry requires that the optical matrix element is proportional to the distance k in k space away from the direct band gap. Both of these cases give rise to allowed transitions in our nomenclature, i.e., exciton transitions can take place for light of infinite wavelength. An extension of Elliott's calculation to two other cases which are of interest for estimating the strengths of various exciton transitions in CdS has been made. The extension is trivial, so only the results will be quoted.

Elliott found that in the case of optical matrix elements proportional to k , the first allowed transitions occur to $2P$ exciton states. In such a case, first forbidden transitions commence with the $1S$ exciton states, and we find that the oscillator strength f_{1S} of a $1S$ state is given in terms of the oscillator strength of a $2P$ exciton

state by

$$\begin{aligned} \frac{f_{1S}}{f_{2P}} &= q^2 |\psi_{1S}(\mathbf{r})|^2_{r=0} / \left| \frac{\partial \psi_{2P_x}(\mathbf{r})}{\partial x} \right|_{r=0}^2 \\ &= 32(a_0q)^2. \end{aligned}$$

Here $\psi(r)$ is a hydrogenic wave function, a_0 is the exciton Bohr radius, and \mathbf{q} is the wave vector of light (having the exciton energy) in the crystal. Similarly, when the band-to-band optical matrix element is quadratic form in k and excludes optical transitions to S states (a situation which can be easily recognized by group theory), optical transitions will be allowed for some $3D$ exciton states, and first forbidden transitions will be allowed to some $2P$ exciton states. For this case

$$f_{2P}/f_{3D} = \left(\frac{3}{2}\right)^9 (a_0q)^2.$$

In CdS, $a_0 \approx 29 \text{ \AA}$, and the wave vector of light in the crystal $= (2\pi/\lambda)(\text{index of refraction}) \approx (300 \text{ \AA})^{-1}$. For either of the two cases considered, the forbidden transitions of a principal quantum number $(n-1)$ have about $\frac{1}{3}$ the strength of the allowed transitions to the allowed state of principal quantum number n .

In order to calculate relative line intensities for the exciton lines under study it would be necessary to calculate the relative magnitude of the first and second order optical matrix elements for the experimental geometry $E||c$. The transition matrix elements, from group theory and $\mathbf{k} \cdot \mathbf{p}$ perturbation theory can be shown to be proportional in lowest order to $(k_x \pm ik_y)$, and in second order to $(k_x \pm ik_y)^2$ and $k_z(k_x \pm ik_y)$. The coefficient of the $(k_x \pm ik_y)$ term is extremely difficult to estimate since it depends critically on the lack of inversion symmetry of the crystal. The coefficient of the $(k_x \pm ik_y)^2$ term is abnormally large because of the near degeneracy of the top two valence bands. We have been able only to conclude from theory alone that either term (or both) could be important.

Unfortunately, the calculation of higher order optical matrix elements depends sensitively on the behavior of the effective-mass wave function near $\mathbf{r}=0$, where it is certain to be in error. Only a few really useful conclusions can be drawn. First, with the exception of the $1S \Gamma_6$ state, all other observable transitions should be either first forbidden or allowed (but not second forbidden) (i.e., with the possible exception of the $1S \Gamma_6$ state, optical matrix elements proportional to powers of q greater than the first power can safely be neglected). For all other states, stronger lines will certainly swamp the second forbidden transitions. Second, only in the $n=2$ states does one expect to see allowed and forbidden processes of comparable strengths. The observable $n=3$ and higher states are certainly allowed, although whether the observed optical strength arises from optical matrix elements proportional to k or k^2 is not known. The existence of both k and k^2 contributions could be responsible for the peculiar behavior of the strength of the continuum transitions noted earlier.

The analysis of the observations has been carried out on the basis of these general conclusions. The most important conclusion is that an observable $n=2$ exciton could have symmetry either Γ_1 or $\Gamma_{\delta y}$. Unfortunately, these conclusions alone are not restrictive enough to lead to a unique interpretation of the experiments.

D. The Orbital Magnetic Effects in Effective-Mass Approximation

A simple canonical transformation on the Hamiltonian (1) when a magnetic field parallel to the hexagonal axis is present results in three magnetic perturbations which can be added directly to (2). The first perturbation is the ordinary Zeeman term,

$$\frac{ieH}{2c} \left(\frac{1}{m_{e\perp}} - \frac{1}{m_{h\perp}} \right) \frac{\partial}{\partial \varphi} \dots, \quad (3)$$

written here in spherical coordinates. The effect of this perturbation is trivial to compute, since φ is a good quantum number even in the presence of the mass anisotropy. It is convenient to define $m(1/m_{h\perp} - 1/m_{e\perp}) \equiv g_{\mu 11}$, and to measure all magnetic moments in units of the free-electron Bohr magneton.

The second perturbation is the ordinary diamagnetic perturbation,

$$\frac{e^2 H^2}{8\mu_{\perp}} (x^2 + y^2) \dots, \quad (4)$$

In order to calculate the effect of (4) correctly to first order in γ , first order wave functions would be necessary. Since the first order corrections will be small, and the experimental accuracy of the diamagnetic shift measurements is low, we have used only the simplest of variational wave functions to compute the effect of (4). The wave functions used were the ordinary orbital wave functions with the exponential factor chosen to minimize the energy. The wave functions thus account in a general way for the change of state radius with binding energy. The expectation values for the term $\langle x^2 + y^2 \rangle$ are

$$\begin{aligned} 1S: 2a_0^2, & & 3P_{\pm 1}: 144a_0^2 \left(1 + \frac{2}{15}\gamma \right), \\ 2S: 28a_0^2, & & 3D_{\pm 1}: 72a_0^2 \left(1 - \frac{2}{21}\gamma \right), \\ 2P_0: 12a_0^2 \left(1 - \frac{4}{15}\gamma \right), & & 3D_{\pm 2}: 108a_0^2 \left(1 + \frac{4}{21}\gamma \right), \\ 2P_{\pm 1}: 24a_0^2 \left(1 + \frac{2}{15}\gamma \right), & & \end{aligned}$$

These coefficients were calculated with the aid of formulas given by Van Vleck.¹³

¹³ J. H. Van Vleck, *The Theory of Electric and Magnetic Susceptibilities* (Oxford University Press, New York, 1932), pp. 178-179.

In addition to these two usual terms, there exists a term⁶

$$\mathbf{r} \cdot [(1/c)\mathbf{v} \times \mathbf{H}] \dots, \quad (5)$$

where \mathbf{r} is the exciton internal coordinate, and \mathbf{v} the exciton velocity as determined by its total mass and wave vector. Since the wave vector of the excitons of interest is the wave vector of light in the crystal at the exciton energy, this term is usually neglected. This term, unfortunately, is not completely negligible for the higher exciton states as will be discussed in Sec. VII.

When the magnetic field is perpendicular to the hexagonal axis, the perturbation terms are not so simple. In the presence of a magnetic field, there will no longer be any good quantum numbers. If the magnetic field is taken in the x direction, the perturbation term linear in the magnetic field will mix the non-degenerate states P_y and P_z . All energy shifts will be second order (or higher) in the magnetic field at low fields. The precise form of the perturbation (although not, of course, the ultimate energies derived) depends on the gauge used. We have chosen a gauge which is slightly asymmetric, the asymmetry chosen in such a way that the coupling by the linear term of the $2P_z$ and $2P_y$ states to $n=3$ states is minimized. (This unwanted coupling vanishes in the symmetric gauge where $\gamma=0$.) In this gauge, the linear perturbation analogous to (3) is

$$\frac{He}{2c} (\mu_{\perp} \mu_{11})^{\frac{1}{2}} \left(\frac{1}{m_{e\perp} m_{e11}} - \frac{1}{m_{h\perp} m_{h11}} \right) (yP_z - zP_y) \dots, \quad (6)$$

having a matrix element between the $2P_y$ and $2P_z$ states

$$\frac{iHe}{c} (\mu_{\perp} \mu_{11})^{\frac{1}{2}} \left(\frac{1}{m_{e\perp} m_{e11}} - \frac{1}{m_{h\perp} m_{h11}} \right) \left(1 + \frac{\gamma}{15} \right) \dots \quad (7)$$

The diamagnetic shifts of the $2P_y$ and $2P_z$ and $2P_x$ states are

$$\begin{aligned} 2P_z \left(1 - \frac{4}{15}\gamma \right) \frac{H^2 e^2}{c^2} 6a_0^2 & \left[\frac{3}{2} \frac{\mu_{\perp}}{\mu_{11}} \frac{1}{(m_{e\perp} + m_{h\perp})} \right. \\ & \left. + \frac{1}{2} \frac{1}{(m_{e11} + m_{h11})} + \frac{\alpha^2}{2\mu_{11}} \right], \\ 2P_y \left(1 + \frac{2}{15}\gamma \right) \frac{H^2 e^2}{c^2} 6a_0^2 & \left[\frac{1}{2} \frac{\mu_{\perp}}{\mu_{11}} \frac{1}{(m_{e\perp} + m_{h\perp})} \right. \\ & \left. + \frac{3}{2} \frac{1}{(m_{e11} + m_{h11})} + \frac{\alpha^2}{2\mu_{11}} \right], \\ 2P_x \left(1 + \frac{2}{15}\gamma \right) \left(\frac{H^2 e^2}{c^2} 3a_0^2 \right) & \left[\frac{\mu_{\perp}}{\mu_{11}} \frac{1}{(m_{e\perp} + m_{h\perp})} \right. \\ & \left. + \frac{1}{(m_{e11} + m_{h11})} + \frac{\alpha^2}{2\mu_{11}} \right] \dots, \end{aligned} \quad (8)$$

where

$$\alpha = \frac{m_{eL}m_{e11} - m_{hL}m_{h11}}{(m_{eL} + m_{hL})(m_{e11} + m_{h11})}$$

All these expressions reduce to the ordinary ones for the case of an isotropic reduced mass. Fortunately, these diamagnetic terms are small enough that the term (7) can be readily extracted from the experimental data without a detailed study of (8). There are, in addition to the terms (8), other diamagnetic terms which should have only a small effect in the gauge chosen. Finally, in the geometry $H \perp c$ there will be quasi-electric field terms analogous to (5).

A magnetic field parallel to the hexagonal axis of the crystal represents a perturbation of symmetry Γ_2 . This perturbation mixes states of symmetry Γ_1 with Γ_2 , Γ_3 with Γ_4 , Γ_5 with itself, and Γ_6 with itself to all orders in perturbation theory. Rigorous optical selection rules still exist in a magnetic field of this symmetry. With the aid of the effective mass theory and the group theoretic classifications of the exciton states, g values for all exciton lines can be simply calculated. (Since the excitons under study have a large radius, direct electron-hole spin-spin coupling is negligible. Because the splitting of the conduction and valence bands away from $\mathbf{k}=0$ is negligible, spin-orbit coupling between the electron or hole spin and the exciton orbital moment is also negligible.) Let g_{e11} and g_{h11} be the g values of the electron and hole, respectively, in this geometry. The g values of all the lines which might possibly be observed in a magnetic field parallel to the c axis are given below.

$1S\Gamma_5, 2S\Gamma_5$	$g = g_{e11} - g_{h11} $,	first forbidden,
$1S\Gamma_6$	$g = g_{e11} + g_{h11} $,	second forbidden,
$2P_0\Gamma_5$	$g = g_{e11} - g_{h11} $,	first forbidden,
$2P_{\pm 1}\Gamma_5$	$g = 2g_{h11} - g_{e11} - g_{h11} $,	first forbidden,
$2P_{\pm 1}(\Gamma_1 + \Gamma_2)$	$g = 2g_{h11} + g_{e11} - g_{h11} $,	allowed,
$3P_{\pm 1}(\Gamma_1 + \Gamma_2)$		
$3D_{\pm 1}(\Gamma_1 + \Gamma_2)$		
$3D_{\pm 2}(\Gamma_1 + \Gamma_2)$	$g = 4g_{h11} - g_{e11} - g_{h11} $,	allowed.

The linear Zeeman effect of the $1S\Gamma_5$ and $2S\Gamma_5$ states is quenched by the longitudinal transverse energy difference, (see Sec. III). Wheeler and Dimmock² have observed quite different diamagnetic shifts for the lines $1S_L$ and $1S_T$ for $H \parallel c$. Their results are readily interpreted as the result of apparent diamagnetic shifts due to the failure of $1S_L$ and $1S_T$ to be degenerate. All other doublets listed should occur as two lines of equal intensity exhibiting a linear splitting with magnetic field.

In a magnetic field perpendicular to the c axis, the linear Zeeman effect on the $1S$ state is again quenched by the longitudinal transverse energy difference. The

same is true to a lesser extent for the $2S$ state, where additional S -state lines become weakly observable in a magnetic field as the magnetic field perturbs the $2S_L\Gamma_5$, $2S_T\Gamma_5$ and $2S\Gamma_6$ states. The analysis of the strengths of the $2P$ lines in this geometry is reserved for Sec. VI.

V. ANALYSIS OF THE OBSERVED ENERGY LEVELS

The analysis of the experimental data, with the aid of the theoretical analysis, is straightforward. The splitting of the higher energy $n=2$ line into four "P" components (two spin doublets) and the lower energy line into only two (one spin doublet) when a magnetic field is applied perpendicular to the c axis, establishes the lower states as P_z and the higher as P_xP_y states. A rydberg of 0.0270 eV and a mass anisotropy γ of 0.222 yields the following set of energy levels, in eV:

State	Theory	Expt.	State	Theory	Expt.
$1S$	0.0270	0.0298	$3P_{\pm 1}$	0.0029	
$2P_0$	0.0071	0.0075	$3D_{\pm 1}$	0.0030	
$2P_{\pm 1}$	0.0065	0.0069	$3D_{\pm 2}$	0.0029	0.0028
$2S$	0.0067		$4P_{\pm 1}$	0.0016	0.0017
$3P_0$	0.0032	$4D_{\pm 1}$	0.0017		
		$4D_{\pm 2}$	0.0016		

The width of the line at 0.0069 eV is 0.0004 eV. The $1S$ state is not expected to be strictly hydrogenic, and should not be used in computing the rydberg. The experimental values have had the origin of energy arbitrarily shifted to facilitate comparison with the theoretical data. Within the accuracy of the calculation, the agreement is adequate. The symmetry of the $n=4$ state has not been established.

The observed $2P_0$ state splits (Fig. 2) into two components in a magnetic field parallel to the c axis. The g value of the Γ_5P_z state should be $|g_{e11} - g_{h11}|$; that of the Γ_6P_z state should be $|g_{e11} + g_{h11}|$. Since only the Γ_5 states should be observed, (see Sec. IV-C) the observed value of $g=0.62 \pm 0.06$ is to be associated with the difference of the g -values. The $1S\Gamma_6$ state has a g value $|g_{e11} + g_{h11}| = 2.93 \pm 0.03$. Since the spin-orbit coupling is thought to be small in CdS and the conduction band simple (and predominantly S -like) we are led to expect the g value of the electron to be near -2.0 . The only g values for electron and hole compatible with this assumption are then

$$g_{e11} = -1.78 \pm 0.05,$$

$$g_{h11} = -1.15 \pm 0.05.$$

The electron g value agrees within experimental error with that determined by Lambe and Kikuchi¹⁴ for chlorine donors in CdS. The $P_{\pm 1}$ states split into four components (in addition to the $2S\Gamma_5$ longitudinal state) in a magnetic field parallel to the c axis. This is precisely what would be expected when both allowed and first forbidden transitions can be seen. The splittings are

¹⁴ J. Lambe and C. Kikuchi, J. Phys. Chem. Solids 8, 492 (1959).

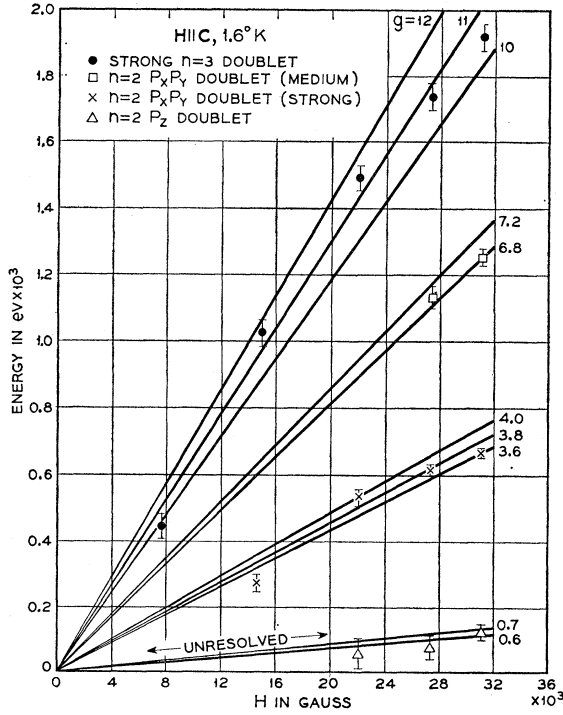


FIG. 7. The separation of the Zeeman doublets for $H||c$. The lack of data at low magnetic fields is due to the failure of many of the lines to be resolved below 20 000 gauss. Compare Figs 2 and 5.

shown in Fig. 2 and Fig. 7. The lack of experimental data at low fields is due to the impossibility of separating the various components until they have been well split by a magnetic field. The more intense line has a g value of 3.8 ± 0.2 ; the weaker line, 6.9 ± 0.2 . There are two possible values of $g_{\mu 11}$ which are compatible with these two g values, as shown below.

	$g_{\mu 11} = -3.30$	$g_{\mu 11} = 2.15$
$g_{\text{allowed line}}$	7.22 ± 0.06	3.67 ± 0.03
$g_{\text{forbidden}}$	3.67 ± 0.03	7.22 ± 0.06

The negative g value (light electron) associates the weaker lines of larger g value with an allowed transition, whereas the choice of a positive g value (a light hole) associates the stronger lines with an allowed transition.

The $n=3$ state splits into two strong components (and several less readily observed weak components) in a magnetic field parallel to the c axis (Fig. 5). The experimental data for the linear splitting is shown in Fig. 7. The g value of this line is 10.8 ± 0.5 .

The $n=3$ $P_{\pm 1}$ and $D_{\pm 1}$ states should exhibit the same g values as the $n=2$ $P_{\pm 1}$ states already discussed. One is thus forced to assume that the observed $n=3$ state is a $3D_{\pm 2}$ state. This is extremely plausible from a theoretical point of view as discussed in Sec. VI. Both of the possible $g_{\mu 11}$ assignments result in the same state assignment for the $n=3$ line, namely a $3D_{\pm 2}(\Gamma_1 + \Gamma_2)$

allowed transition. One obtains for the predicted g values:

$g_{\mu 11}$	$g(3D_{\pm 2} \text{ allowed transition})$
-3.30	10.27
+2.15	11.53

Section VII shows that there is reason to believe that a small but measurable error exists in interpreting the experimental g values at face value; hence one is forced to conclude from the $H||c$ data alone that either value of $g_{\mu 11}$ could be regarded as an acceptable fit to the experimental data. From the dielectric constants $\epsilon_L = 9.02$ and $\epsilon_{11} = 9.53$ (determined by Berlincourt *et al.*¹⁵ at frequencies above the thickness shear resonance) and the binding energy, one finds $\mu_L = 0.160$, $\mu_{11} = 0.190$. The two sets of $g_{\mu 11}$ permit two choices of electron and hole masses. If $g_{\mu 11} = -3.30$, $1/m_{eL} = 4.78$ and $1/m_{hL} = 1.48$. If $g_{\mu 11} = +2.15$, $1/m_{eL} = 2.06$ and $1/m_{hL} = 4.20$.

The splitting of the $2P$ states for a magnetic field perpendicular to the hexagonal axis is quite simple. The hole (from group theory) has no resolvable magnetic moment in this geometry (i.e., $H||x$ is Γ_{5y} and thus does not mix Γ_9 with itself). If the magnetic field is in the x direction, the state P_x undergoes a diamagnetic shift and the states P_y and P_z will (although not degenerate) repel each other with an effective g value

$$g_L = 2(\mu_L \mu_{11})^{\frac{1}{2}} \left(\frac{1}{m_{hL} m_{h11}} - \frac{1}{m_{eL} m_{e11}} \right) \left(1 + \frac{\gamma}{15} \right).$$

The P_y and P_z states also undergo a diamagnetic shift, but this shift can be essentially eliminated from the analysis of the value of g_L . Finally, each of the states P_x, P_y, P_z is split into a doublet having a splitting g_{eL} . An analysis of the data of Fig. 3 yields $|g_{eL}| = 1.72 \pm 0.1$, (also in agreement with Lambe and Kikuchi) and $|g_L| = 8.3 \pm 0.3$. Since it is impossible to determine *a priori* the sign of g_L , we are led finally to four sets of electron and hole mass values A, B, C , and D as given below:

	m_{eL}	m_{hL}	m_{e11}	m_{h11}
A	0.209	0.68	0.198	5.0
B	0.209	0.68	-0.339	0.122
C	0.485	0.238	0.120	-0.322
D	0.485	0.238	-3.33	0.180

There are several independent arguments, which give information concerning the most reasonable choice of mass values. First, the "reasonable" assumption based on Sec. IV that the $2P$ allowed transitions should be stronger than the $2P$ forbidden transitions would necessitate the choice of C or D . However, the direct demonstration in Sec. VI that the forbidden $2P_{\pm 1}$ is stronger than the allowed $2P_{\pm 1}$ transition is strong

¹⁵ D. Berlincourt, H. Jaffe, H. Krueger, and L. Shiozawa (to be published).

evidence for choice *A* or *B*. Second, the fact that excitons from the top two valence bands have the same binding energy¹ is most easily explained by arguing that the dominant contribution to the reduced mass in both directions is the electron; i.e., that the electron is lighter than the hole in both directions. This argument favors choice *A*. Third, the small anisotropy of the reduced mass is physically understandable in choice *A* or *D*, for one particle is light and isotropic, and the sizable anisotropy of the other particle then produces a small reduced-mass anisotropy. The other mass choices result in a small reduced-mass anisotropy by the near cancellation of large mass anisotropies of holes and electrons. Fourth, the failure of Thomas, Hopfield, and Power¹⁶ to observe indirect transitions suggests that the conduction band minimum and valence band maximum used to construct the excitons under study are absolute maxima and minima or very nearly so. This argument, which is not definitive, may be taken as evidence against the occurrence of small negative masses, and argues against choices *B*, *C*, and perhaps *D*. Fifth, preliminary experiments by Collins¹⁷ on the infrared reflectivity minimum of highly doped CdS indicate that the mass of the conduction electrons is about 0.2 and isotropic. The absence of indirect transitions may be taken as evidence that the electron mass in the exciton should be the same. This argument is in good agreement with the set of masses *A*. Finally, $\mathbf{k} \cdot \mathbf{p}$ perturbation theory applied to a simple band model which takes into account only the conduction band and the three known valence bands suggests that the electron is isotropic and lighter than the hole. This theory further suggests that for an electron mass $1/m_e = 5$, the hole masses should (very approximately) obey the relation $1/m_{hL} = 2 + 1/m_{hH}$, the reason for the hole mass anisotropy is that the top valence band is composed of P_x and P_y states only, and is not repelled by the *S*-like conduction band for a $\mathbf{k} \cdot \mathbf{p}$ perturbation in the *z* direction. The mass assignment *A* is in good qualitative agreement with the naive $\mathbf{k} \cdot \mathbf{p}$ perturbation theory, while other mass assignments are in qualitative disagreement.

Thus the bulk of the direct and indirect evidence seems to support strongly choice *A*.

The agreement between experiment and theory with masses *A* in the geometry $H \perp c$ is exhibited in Fig. 3, where the solid lines represent the theoretical mass assignments. Agreement is generally quite good.

The agreement between theory and experiment for the measured *g* values for $H \parallel c$ is shown by the scatter of the experimental points in Fig. 7 about the solid lines (theoretical fit). Considering the sources of systematic error (Sec. VII), agreement is generally as good as could be expected.

¹⁶ D. G. Thomas, J. J. Hopfield, and M. Power, Phys. Rev. **119**, 570 (1960).

¹⁷ R. J. Collins (private communication).

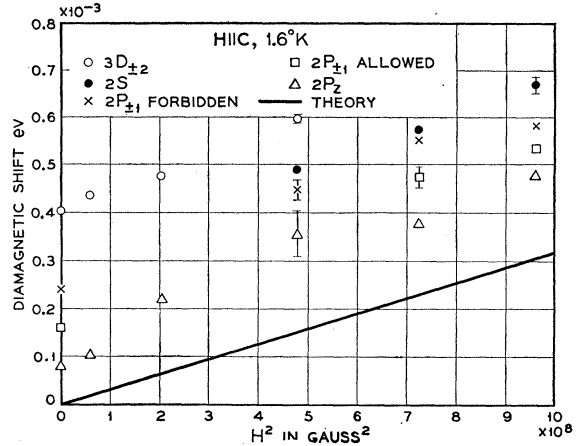


Fig. 8. The diamagnetic shift of the $2P$, $2S$, and $3D$ states for $H \parallel c$. The data for each exciton line should lie along a line parallel to (but not coincident with) the theoretical line. An estimated scaled experimental uncertainty is indicated for a point from each exciton line.

The agreement between theory and experiment for the diamagnetic shifts is difficult to assess. For the $n=2$ states, the diamagnetic shift is difficult to measure with high precision. For the $n=3$ states, the diamagnetic shift at large magnetic fields (above 20 000 gauss) should no longer be proportional to H^2 . The diamagnetic shift for all exciton lines has been reduced to a common basis in Fig. 8. The diamagnetic data for each line should lie along a straight line parallel to but not coincident with the theoretical solid line. The theoretical line unfortunately also may be in error, since its slope is proportional to ϵ^{-4} , and the precision of measurement of ϵ is only 2 or 3%. In addition, the quasi-electric field (Sec. VII) will affect the apparent diamagnetic shift.

A rydberg of 0.0290 eV yields better over-all agreement with the observed energy level spacings than the rydberg used in the present calculations, 0.0270 eV. The rydberg of 0.0270 eV is in much better accord with the diamagnetic shifts observed. The uncertainty of the effective rydberg is the largest source of uncertainty in the calculation of the masses.

The actual limits of error of the masses are almost impossible to assess. The internal consistency of the interpretation, assuming no error in the dielectric constant, is compatible with an estimated error of ± 0.25 for any calculated reciprocal mass. A different dielectric constant would, of course, alter our estimate of internal consistency. The calculated electron mass is then isotropic within experimental error, and is $m_e = 0.204 \pm 0.010$. The calculated hole masses are $m_{hL} = 0.7 \pm 0.1$, and $m_{hH} = 5$, the limits for m_{hH} being $m_{hH} > 2.2$ if m_{hL} is positive, and $m_{hH} < -20$ if m_{hL} is negative. Because the exciton states are weakly bound, the calculated masses are polaron masses, not bare masses. The electron "bare" mass should be about 10% lighter than the value deduced here.

VI. OBSERVATION OF FORBIDDEN TRANSITIONS

The observation of more exciton lines of principal quantum number $n=2$ than is expected from group theory indicates that forbidden transitions can occur for $n=2$ exciton states. This argument is not definitive, since other effects (such as strain) could also cause the breakdown of selection rules.

It has been observed⁶ (see also Sec. III) that the magneto-optic absorption spectrum of the $2P$ exciton states alters drastically when the magnetic field is reversed when the geometry $q \perp H$, $E \parallel c$, $H \perp c$ is used. Since time reversal reverses the sign of the magnetic field but leaves the selection rules for infinite wavelength linearly polarized light (in a crystal of any symmetry whatsoever) invariant, one is forced to conclude that the effect must be due to the finite wave vector of light and the excitons with which the light interacts. In a crystal with inversion symmetry, even the finite wave vector of light cannot give rise to this effect. The wurtzite structure, however, has a direction to the c axis and thus lacks inversion symmetry.

Consider a geometry in which the magnetic field is in the $+x$ direction and the wave vector of the light q in the $+y$ direction.

The energy levels are those of the third column of Fig. 9. Each "spin doublet" is split by the electron g value g_{el} . The top pair of lines is mixed with the bottom pair of lines by the magnetic interactions analyzed quantitatively in Sec. V. The energy levels will be independent of the direction of H relative to q_y as long as H is perpendicular to the c axis, and so are the same for $H_x = -H_x$ (4th column of Fig. 9) and $H \parallel q_y$ (5th column). The zero field line pattern and the splitting of the exciton states for $H \parallel c$ is given in the first two columns for reference.

It is observed experimentally [Figs. 1(a) and 1(b)] that the top line of each doublet tends to be strong (in the geometry $H \perp q_y$, $H \perp c$) with the magnetic field in one direction ($H \times q \cdot c > 0$) and to be weak (and the lower line strong) when the magnetic field is reversed. It has already been indicated that such effects cannot occur (in linearly polarized light) for allowed transitions. It will now be shown that these effects can be

quantitatively explained with the inclusion of forbidden transitions.

The states can be described as factored orbital and spin wave functions. Let the direction of spin quantization be chosen as the z direction. A typical exciton state could be written $P_x \uparrow_e \downarrow_h$, with the interpretation that the exciton orbital wave function is a $2P_x$ effective mass state, the electron spin is in the z direction, and the empty state in the valence band is a state in which the electron spin would be oriented in the $-z$ direction.

The optical matrix elements of the states in the presence of a magnetic field are easily computed from the symmetry combinations of allowed and first forbidden matrix elements. The state

$$\frac{1}{2}(P_x + iP_y) \uparrow_e \uparrow_h + \frac{1}{2}(P_x - iP_y) \downarrow_e \downarrow_h$$

is a Γ_1 state and has an optical matrix element A independent of the propagation vector $q = q_y$ of the light. This state combines with a Γ_2 state to produce the allowed $2P_{\pm 1}$ doublet in a magnetic field parallel to the c axis. Each component of this doublet will have a strength $\frac{1}{2}|A|^2$ (in appropriate units). The state

$$\frac{1}{2}(P_x + iP_y) \downarrow_e \uparrow_h + \frac{1}{2}(P_x - iP_y) \uparrow_e \downarrow_h$$

has the symmetry Γ_{5y} and an optical matrix element qB . In a magnetic field parallel to the c axis this state mixes with the corresponding Γ_{5x} state to form the forbidden $P_{\pm 1}$ doublet, each component having the strength $\frac{1}{2}|q_y B|^2$. The state

$$\frac{1}{\sqrt{2}} P_z (\uparrow_e \uparrow_h - \downarrow_e \downarrow_h)$$

is also a Γ_{5y} state having an optical matrix element qC . This state combines with its analogous Γ_{5x} state to produce the P_0 doublet for $H \parallel c$, each component having the strength $\frac{1}{2}|qC|^2$. All other optical matrix elements are proportional at least to q_y^2 and will be neglected.

From the eigenstates in an applied magnetic field, the line strengths of any of the geometries can be easily computed in terms of these three matrix elements. For example, for H in the $+x$ direction, one finds for states

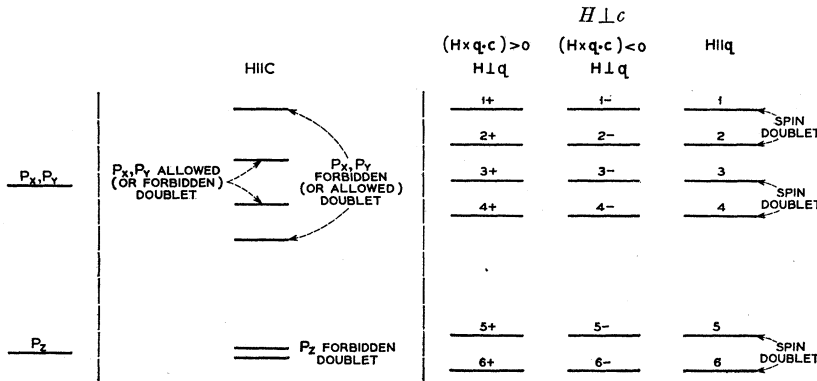


FIG. 9. The energy level scheme (schematic) for the $2P$ exciton states without magnetic field and in the presence of magnetic fields in several directions.

(3+), (4+), (3-), and (4-),

$$\begin{aligned}
 (3+) \left\{ \begin{array}{l} (1/\sqrt{2})P_x[\uparrow_e + \downarrow_e]\uparrow_h \\ (1/\sqrt{2})P_x[\uparrow_e + \downarrow_e]\downarrow_h \end{array} \right\} &: \text{total strength} \\
 &= \frac{1}{4}|A+qB|^2, \\
 (4+) \left\{ \begin{array}{l} (1/\sqrt{2})P_x[\uparrow_e - \downarrow_e]\uparrow_h \\ (1/\sqrt{2})P_x[\uparrow_e - \downarrow_e]\downarrow_h \end{array} \right\} &: \text{total strength} \\
 &= \frac{1}{4}|A-qB|^2, \\
 (3-) \left\{ \begin{array}{l} (1/\sqrt{2})P_x[\uparrow_e - \downarrow_e]\uparrow_h \\ (1/\sqrt{2})P_x[\uparrow_e - \downarrow_e]\downarrow_h \end{array} \right\} &: \text{total strength} \\
 &= \frac{1}{4}|A-qB|^2, \\
 (4-) \left\{ \begin{array}{l} (1/\sqrt{2})P_x[\uparrow_e + \downarrow_e]\uparrow_h \\ (1/\sqrt{2})P_x[\uparrow_e + \downarrow_e]\downarrow_h \end{array} \right\} &: \text{total strength} \\
 &= \frac{1}{4}|A+qB|^2.
 \end{aligned}$$

The energies are independent of hole orientation for $H \perp c$ ($g_{h\perp}=0$). All energy states are therefore doubly degenerate, and the intensity observed is the sum of the two degenerate line intensities. The causes of the change in intensity at a given energy position (for example that of state 3) with reversal of the magnetic field is now clear. If A and B have the same (or nearly the same) complex phase, the allowed and forbidden amplitudes for states (3+) and (4-) add, and for (4+) and (3-) subtract. Thus reversal of the magnetic field should interchange the intensities observed in line positions (3) and (4). Since reversal of the direction of propagation of light reverses the sign of q , reversal of the direction of propagation of the light should also interchange the intensities observed at lines (3) and (4). Both of these effects have been observed experimentally. Theory and experiment agree that reversing both H and q will not alter the observed intensities.

The intensities of all other lines can be found in a similar manner. It is necessary to make an arbitrary choice of the sign of the $g_{e\perp}$ value for the electron, g_e , and the geometry defined by $\mathbf{H} \times \mathbf{q} \cdot \mathbf{c} > 0$. All choices are equivalent under suitable choice of signs of A , B , and C , and produce the same theoretical fit to experiment. The intensities of most of the lines contain a parameter β . Since the P_{xy} and P_x states are not degenerate, the linear combinations of P_y and P_z which will enter into an eigenstate when the magnetic field is parallel to the x axis will depend on the magnitude of the magnetic field. One orbital eigenstate can be defined as

$$(1-\beta^2)^{\frac{1}{2}}P_y + i\beta P_z,$$

with β positive. The value of β as a function of the magnetic field is easily computed from the analysis of the energy levels in this geometry performed in Sec. V. From this analysis, one obtains the expression

$$\beta = \sin \left\{ \tan^{-1} \left(\left[\left(\frac{1.33}{H} \right)^2 + 1 \right]^{\frac{1}{2}} - \frac{1.33}{H} \right) \right\},$$

where H is the magnetic field in units of 10^4 gauss. For

TABLE III. Theoretical expressions for the intensities of the $2P$ exciton lines in various magnetic geometries.

State	Intensity
$H \parallel c$	
$2P_{\pm 1}$ (allowed)	$\frac{1}{2} A ^2$ (each line)
$2P_{\pm 1}$ (forbidden)	$\frac{1}{2} qB ^2$ (each line)
$2P_x$ (forbidden)	$\frac{1}{2} qC ^2$ (each line)
$H \perp c$	
(1+)	$\frac{1}{8} \sqrt{2}(1-\beta^2)^{\frac{1}{2}}(A+qB) - 2\beta qC ^2$
(2+)	$\frac{1}{8} \sqrt{2}(1-\beta^2)^{\frac{1}{2}}(A-qB) - 2\beta qC ^2$
(3+)	$\frac{1}{4} A+qB ^2$
(4+)	$\frac{1}{4} A-qB ^2$
(5+)	$\frac{1}{8} \beta\sqrt{2}(A+qB) + 2(1-\beta^2)^{\frac{1}{2}}qC ^2$
(6+)	$\frac{1}{8} \beta\sqrt{2}(A-qB) + 2(1-\beta^2)^{\frac{1}{2}}qC ^2$
(1-)	$\frac{1}{8} \sqrt{2}(1-\beta^2)^{\frac{1}{2}}(A-qB) + 2\beta qC ^2$
(2-)	$\frac{1}{8} \sqrt{2}(1-\beta^2)^{\frac{1}{2}}(A+qB) + 2\beta qC ^2$
(3-)	$\frac{1}{4} A-qB ^2$
(4-)	$\frac{1}{4} A+qB ^2$
(5-)	$\frac{1}{8} \beta\sqrt{2}(A-qB) - 2(1-\beta^2)^{\frac{1}{2}}qC ^2$
(6-)	$\frac{1}{8} \beta\sqrt{2}(A+qB) - 2(1-\beta^2)^{\frac{1}{2}}qC ^2$
(1)	$\frac{1}{4}[(1-\beta^2) A ^2 + (1-\beta^2)^{\frac{1}{2}}qB - \sqrt{2}\beta qC]^2$
(2)	$\frac{1}{4}[(1-\beta^2) A ^2 + (1-\beta^2)^{\frac{1}{2}}qB + \sqrt{2}\beta qC]^2$
(3)	$\frac{1}{4}[A ^2 + qB ^2]$
(4)	$\frac{1}{4}[A ^2 + qB ^2]$
(5)	$\frac{1}{4}[\beta^2 A ^2 + \beta qB + (1-\beta^2)^{\frac{1}{2}}\sqrt{2}qC ^2]$
(6)	$\frac{1}{4}[\beta^2 A ^2 + \beta qB - (1-\beta^2)^{\frac{1}{2}}\sqrt{2}qC ^2]$

low magnetic fields, β is proportional to the magnetic field, and achieves asymptotically the value $1/\sqrt{2}$ for large fields. At 31 000 gauss, $\beta=0.55$.

Expressions for the strengths of all the $2P$ exciton states as a function of geometry, and of the quantities A , B , and C are given in Table III. In the geometry $H \parallel q$, theory and experiment agree that no alterations of line intensity with the reversal of \mathbf{H} or \mathbf{q} will occur. For this reason only one set of values is needed in this geometry.

The matrix elements A , B , and C are in general complex, so five theoretical constants are to be determined by a fit to experiment. Since only the relative phase of A , B , and C enters the calculation, a sixth constant may be chosen arbitrarily to define the absolute phase of A , B , and C . For convenience, we have picked B to be real. The strengths of $2P_{\pm 1}$ (allowed), $2P_{\pm 1}$ (forbidden), $2P_x$ (forbidden), (5-), and (6-) have been used to determine the five constants. One finds, in arbitrary experimental units

$$A = 2.1 + 2.3i,$$

$$qB = 4.1,$$

$$qC = 1.0 - 1.3i.$$

The calculated intensities of all twenty-one $2P$ exciton states observed in different magnetic field geometries are compared with the experimental intensities in Table VI. In general, the agreement is excellent.

The most surprising result of this fit to the experi-

TABLE IV. A comparison of calculated and experimental values for the strengths of the $2P$ exciton states in different magnetic field geometries. The experimental values are from photographic plates and are approximate, they are taken to be proportional to the values of αt at the peak of the appropriate absorption line. For convenience the sum of the line strengths for $H \parallel c$ has been set equal to 30 and so the sum of the theoretical strengths of each set of lines for all geometries is also 30. There is a theoretical sum rule that for all geometries with $H \perp c$, $1+2+5+6 = \frac{1}{2}\{(2P_{\pm 1}) \text{ allowed} + (2P_{\pm 1}) \text{ forbidden}\} + (2P_z)$, which in this case is $\approx (5.1+8.4+2 \times 1.4) = 16.3$. This sum rule was used to normalize each set of experimental results for $H \perp c$.

State	Theoretical intensity ($H=31\,000$ gauss)	Measured intensity
$H \parallel c$		
$2P_{\pm 1}$ (allowed)	5.1 (each line)	4.9
$2P_{\pm 1}$ (forbidden)	8.4 (each line)	8.6
$2P_z$	1.4 (each line)	1.4
$H \perp c$		
(1+)	6.8	5.8
(2+)	3.6	3.9
(3+)	10.9	$> 9.1^a$
(4+)	2.4	3.2
(5+)	6.8	6.6
(6+)	0.0	< 0.1
$q \perp H$		
(1-)	0.5	< 0.1
(2-)	8.9	8.2
(3-)	2.4	6.6 ^a
(4-)	10.9	> 7.8
(5-)	3.3	4.0
(6-)	3.3	3.9
$q \parallel H$		
(1)	3.7	2.5
(2)	6.4	6.4
(3)	6.8	$> 8.0^a$
(4)	6.8	7.0
(5)	4.4	5.8
(6)	1.6	1.5

^a These states cannot be separated from the $2S_L$ state; consequently the indicated line strength may be greater than that of the $2P_z$ state alone.

mental data is the fact that it assigns the strongest $2P$ transitions to forbidden processes. It is not possible to obtain even a satisfactory qualitative fit to the experimental data unless the strongest transitions are assigned as forbidden. The strong forbidden transitions are in agreement with the mass analysis of Sec. V, in which all the circumstantial evidence indicated that the strong $2P$ transitions must be forbidden.

Figure 10 shows the experimental and theoretical intensities of lines (5-) and (6-) as a function of magnetic field. The depth and position of the minimum of intensity of line (6-) is a very sensitive function of the optical matrix elements. In view of the relatively large experimental errors in determining the line intensity ratios from which A , B , and C were determined, the agreement between experiment and theory can be considered adequate. Experiment and theory agree that the equality of the intensities of lines (5-) and (6-) for a magnetic field of 31 000 gauss is accidental, and does not occur for other magnetic fields.

In Sec. IV, it was estimated that the forbidden $2P$ transitions should be about $\frac{1}{3}$ the strength of the allowed

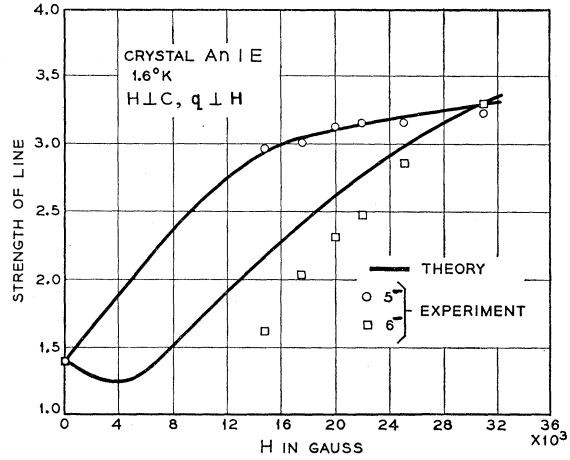


FIG. 10. The theoretical and experimental strengths of the (5-) and (6-) lines as a function of magnetic field. The line strengths are in units of αt , where α is the peak absorption coefficient in cm^{-1} and t , the crystal thickness, is 10μ . Experimental data are not given below 15 000 gauss since in this region the two lines cannot be resolved.

$3D$ transitions. Experiment shows that this is at least approximately so.

That the $2P_0$ forbidden lines are much weaker than the $2P_{\pm 1}$ lines is consistent with the experimental observation of $3D_{\pm 2}$ allowed transitions but not $3D_{\pm 1}$ allowed transitions. One can easily show, following the analysis of Sec. IV, that the strengths of the $2P_{\pm 1}$ forbidden transition is related to the strength of the $3D_{\pm 2}$ allowed transitions by almost the same factor that related the strength of the $2P_0$ forbidden transition and the $3D_{\pm 1}$ allowed transition. That the $2P_{\pm 1}$ allowed transition is weak in spite of the near degeneracy of this state from the top valence band and the strong $1S$ transition from the second valence band indicates that the optical matrix element between the top two valence bands at $k=0$ is truly infinitesimal.

Perhaps the most disconcerting aspect of the explanation of the anomalous magneto-optic absorption spectrum is that its observation, although theoretically plausible, appears to be accidental. The accidental nature of the phenomenon is clear from the fact that it depends on the magnetic mixing of two exciton states of different symmetry by a magnetic field. The phenomenon thus depends on the accidental near degeneracy of two exciton states.

A few simple criteria must be met in order to observe this type of magneto-absorption spectrum in wurtzite CdS, ZnS, ZnO, etc. First, one must be able to observe a forbidden exciton absorption line, whose strength will be denoted by I_f . Second, there must lie a distance ϵ away an allowed exciton absorption line, whose strength will be denoted by I_a . (The spin-orbit splitting of the valence band must be greater than $\mu_B H$, but this is true for virtually all crystals.) Third, there must be a magnetic coupling between the allowed and forbidden transitions.

When this coupling exists, it will usually have an approximate magnitude $\mu_B H$. All that is required in order to have the possibility of observing the strange magnetic-field reversal effects (symmetry permitting) is that $\mu_B H$ be of the same order of magnitude as $(I_f/I_a)^{1/2}\epsilon$. The quantity $(I_f/I_a)^{1/2}$ ranges from about 1 to 10^{-2} . The accidental degeneracy is, for hydrogenic or near hydrogenic excitons, extremely close, and ϵ will typically lie, depending on the states involved, between 10^{-2} and 10^{-5} ev. $\mu_B H$ for customary laboratory fields is about 2×10^{-4} ev.

For the $2P$ CdS exciton states, ϵ lies between 10^{-3} and 10^{-4} ev, a perfectly reasonable and unexceptional value. One would then expect, if a forbidden $2P$ exciton line can be observed at all, to be able to observe magnetic field reversal effects for any value of (I_f/I_a) likely to occur in nature. The only accident that occurs in CdS is that $(I_f/I_a)^{1/2}$ is near 1, making the interference effects particularly marked. The anomalous magnetic field reversal effect observed in CdS is thus expected to occur in the exciton spectrum of most of the II-VI wurtzite structure compounds when properly selected exciton lines are carefully investigated.

VII. PERTURBATIONS

A. The Effect of the Quasi-Electric Field

The magnetic perturbation (5), neglected throughout the previous analysis, is equivalent to an applied electric field perpendicular to \mathbf{q} and \mathbf{H} . This quasi-field has a magnitude of approximately 100 volts/cm for the excitons under consideration and a magnetic field of 31 000 gauss. In the absence of all other magnetic effects and effects of anisotropy, this quasi-field would produce a Stark effect linear in H . This effect would give rise to a maximum splitting interpretable as a "g value" of about 1 for the $n=2$ states, and 3 for the $n=3$ states in CdS.

Fortunately, in the presence of anisotropy and sizable ordinary magnetic effects the contribution of this Stark effect to the ordinary splittings is much reduced by the destruction of degeneracy. The maximum effect on the $n=2$ states is expected to be of the same magnitude as present experimental error. On the $3D_{\pm 2}$ states the "Stark effect" should lead to an increase of about 10% in the measured g value over the true g value. The experimental data were not corrected for this effect.

B. The Effect of a Finite Slope Conduction Band at $k=0$

Casella⁸ has pointed out that the conduction band in CdS need not be degenerate away from the line $k_x=k_y=0$. More recently, Balkanski and des Cloizeaux⁹ have given an interpretation of some of the optical absorption effects in CdS on the basis of a sizable slope band crossing in the conduction band at $\mathbf{k}=0$. The

magnetic effects on the $2P$ excitons are quite sensitive to the presence of a finite slope band crossing. All the $2P_{xy}$ exciton states are degenerate in the effective mass approximation in the absence of valence and conduction band splittings away from $\mathbf{k}=0$. The presence of a finite slope conduction band crossing, even in the effective mass approximation, would mix the $2S\Gamma_6$ and $2P_{\pm 1}\Gamma_5$ states, altering the energy of the $2P_{\pm 1}\Gamma_5$ state. The $2P_{\pm 1}\Gamma_1$ state would behave differently, since there is no $2S$ state of the same symmetry. The splitting of the $2P_{\pm 1}\Gamma_1$ and $2P_{\pm 1}\Gamma_5$ states was computed in lowest order, for a finite slope conduction band crossing. The degeneracy (within the experimental error of perhaps 0.3 millielectron volt) of all the $2P_{xy}$ excitons regardless of symmetry gives an upper limit on the slope at the band crossing at $\mathbf{k}=0$ of

$$|dE/dk|_{k=0} < 5 \times 10^{-10} \text{ electron-volt centimeter.}$$

This estimate is at least an order of magnitude smaller than that which would have to be assumed by Balkanski and des Cloizeaux. A perturbation of this symmetry ten times larger would have drastic effects on the exciton spectrum, and could scarcely be overlooked. The valence band splitting proportional to k^2 should be similarly insignificant.

C. The Use of the Effective-Mass Approximation

The analysis has been carried out on the basis of a single valence band and the effective-mass approximation. Since the ground-state exciton has a binding energy of 0.027 ev and the valence band separation at $\mathbf{k}=0$ is only 0.016 ev, it is clear that effects of the other valence bands are not completely negligible. The magnitude of the effect of the other valence bands on the effective-mass energy levels cannot be calculated from presently known parameters. As in the case of the finite-slope band crossing, the fact that the $2P$ states show the full effective-mass degeneracy shows that the other valence bands do not seriously perturb the $n=2$ states. The fact that the $1S\Gamma_6$ state and the $2P\Gamma_5$ states combine to yield a value of g_{e11} in agreement with other experiments (see Sec. V) may be interpreted as indicating that the g value of the $1S\Gamma_6$ state is not seriously perturbed. This does not, unfortunately, guarantee that its energy has not been shifted appreciably.

VIII. CONCLUSION

The energy levels of the excitons in CdS formed from the top valence band and the conduction band are well represented by the effective-mass approximation. The reduced mass of the exciton is only slightly anisotropic. In the presence of a magnetic field, it is possible in light polarized parallel to the hexagonal axis to observe sufficient g values to calculate with the aid of group theory the g values of the electron and hole and the masses of the electron and hole. The mass assignment

which agrees most satisfactorily with all experiments and theoretical considerations are (in units of the free electron mass)

$$m_e = 0.205 \text{ (isotropic within 5\%)}, \quad m_{h11} \sim 5,$$

and

$$m_{h1} = 0.7.$$

Comparison of the present results with other experiments supports the suggestion that the $\mathbf{k}=0$ conduction band valley is the lowest conduction band valley in CdS. The slope of the conduction band at $\mathbf{k}=0$ and the displacement of the conduction band minimum from $k_x = k_y = 0$ appear to be negligible.

Piper *et al.*¹⁸ have suggested from transport measurements that 0.03 eV represents the binding energy of a hydrogen-like donor in CdS. The donor state binding energy of 0.033 eV computed from the electron effective mass and the static dielectric constants is in reasonable agreement with the observed value. Naive application of the theory of Luttinger and Kohn¹⁹ for the computation of the hydrogenic acceptor state binding energy, using the hole masses from the top valence band, leads to a binding energy of 0.4 eV. Correctly taking into account the lattice polarizability and the fact that the acceptor state binding energy is much larger than the $\mathbf{k}=0$ valence band splittings, will increase the acceptor binding energy. From this calculation one would suggest that the ground state of all hole traps for which a hole, at long range, feels an attractive Coulomb force (such as an ionized acceptor) should have a binding energy greater than 0.4 eV. The central cell correction will control the actual binding energy for such a trap. Optical experiments usually indicate that acceptor binding energies are of the order of 1 eV, in qualitative agreement with what might be expected. It is also of interest that the hole mobility

in the top valence band is expected to be highly anisotropic, with $\mu_x/\mu_{11} \approx 6$ for an isotropic relaxation time.

In order to understand the number of observable exciton lines, it is necessary to assume that optical transitions having an optical matrix element proportional to the wave vector of the light are of fundamental importance. These first forbidden transitions are necessary to explain the large changes in some magneto-optic absorption spectra when the magnetic field is reversed. A theory taking into account both allowed and forbidden optical transitions explains quantitatively this peculiar absorption spectrum. Theoretical support for the existence of large optical matrix elements for forbidden transitions also was given.

Small effects of the quasi-electric field acting on an exciton due to its motion through a uniform magnetic field have been observed. These effects are sufficiently large that the direct measurement of the exciton mass ($m_{e1} + m_{h1}$) should be possible in CdS. They also give rise to sizable systematic error if the g values of $n=3$ and higher exciton states in CdS are interpreted as being the g values characteristic of excitons having zero wave vector.

Unambiguous evidence for the quenching of a Zeeman effect by lifting of a "group-theoretic" degeneracy by the energy difference between longitudinal and optically active excitons was observed.

ACKNOWLEDGMENTS

The authors would like to thank Dr. W. W. Piper of the General Electric Company Research Laboratory and Dr. D. C. Reynolds of the Wright-Patterson Air Force Research Center for the crystals used in these experiments. They also wish to thank Dr. R. J. Collins for allowing us to use his unpublished measurements of the free carrier effective mass, and Dr. D. Berlincourt for his measurements of the dielectric constants. Thanks are also due to Mr. E. A. Sadowski for much technical assistance.

¹⁸ W. W. Piper *et al.*, International Conference at Prague, August, 1960 (to be published).

¹⁹ W. Kohn and J. M. Luttinger, Phys. Rev. **98**, 915 (1955).